

# Interband Recombination Dynamics in Resonantly-Excited Single-Walled Carbon Nanotubes

G. N. Ostojic, S. Zaric, J. Kono\*

*Department of Electrical and Computer Engineering, Rice Quantum Institute,  
and Center for Nanoscale Science and Technology, Rice University, Houston, Texas 77005*

M. S. Strano, V. C. Moore, R. H. Hauge, R. E. Smalley

*Department of Chemistry, Rice Quantum Institute,  
and Center for Nanoscale Science and Technology, Rice University, Houston, Texas 77005*

(Dated: October 29, 2018)

Wavelength-dependent pump-probe spectroscopy of micelle-suspended single-walled carbon nanotubes reveals two-component dynamics. The slow component (5-20 ps), which has not been observed previously, is resonantly enhanced whenever the pump photon energy coincides with an absorption peak and we attribute it to interband carrier recombination, whereas we interpret the always-present fast component (0.3-1.2 ps) as intraband carrier relaxation in non-resonantly excited nanotubes. The slow component decreases drastically with decreasing pH (or increasing  $H^+$  doping), especially in large-diameter tubes. This can be explained as a consequence of the disappearance of absorption peaks at high doping due to the entrance of the Fermi energy into the valence band, i.e., a 1-D manifestation of the Burstein-Moss effect.

PACS numbers: 78.47.+p, 78.67.Ch, 73.22.-f

Optical properties of one-dimensional (1-D) systems have been the subject of numerous theoretical studies for many years [1]. Various 1-D systems have been investigated experimentally, but the distinct characters of 1-D excitons have not been revealed unambiguously. Single-walled carbon nanotubes (SWNTs) [2] provide a viable alternative for exploring 1-D exciton physics, and, in addition, they are expected to show a new class of optical phenomena that arise from their unique tubular structure. Linear and nonlinear optical coefficients are expected to be diameter- and chirality-dependent, and a magnetic field applied parallel to the tubes is expected to induce non-intuitive modifications on their electronic, magnetic, and optical properties via the Aharonov-Bohm phase [3]. Furthermore, high-order harmonic generation is expected to be extremely selective [4].

However, these theoretical predictions are mostly unexplored experimentally. The main reason is that SWNTs easily form bundles (or ‘ropes’), consisting of different tube types, due to their strong van der Waals forces. This results in significant broadening, smearing out any chirality-dependent features [5]. Very recently, a new technique for producing individually-suspended SWNTs in solutions has been reported [6]. It consists of separating tubes by vigorous sonication, followed by micelle wrapping of individual tubes to prevent bundling. These samples have revealed, for the first time, a number of clearly observable peaks in linear absorption and photoluminescence (PL) spectra, corresponding to interband transitions in different types of tubes. Subsequent photoluminescence-excitation (PLE) spectroscopy studies successfully provided detailed peak assignments [7, 8].

Here we report results of wavelength-dependent pump-probe spectroscopy on such micelle-suspended and

chirality-assigned SWNTs. Unlike the bundled nanotubes used in previous pump-probe experiments [9, 10, 11, 12], our samples show distinct interband absorption and PL peaks (see Fig. 1). By scanning the photon energy in a wide range, we were able to identify different types of relaxation processes. Specifically, we discovered two distinct relaxation regimes: fast (0.3-1.5 ps) and slow (5-20 ps). The slow component, which has not been observed previously, is *resonantly enhanced* whenever the pump photon energy coincides with an absorption peak, and we ascribe it to interband carrier recombination in resonantly-excited nanotubes. The fast component is always present, and we attribute it to intraband carrier relaxation in non-resonantly-excited nanotubes. Furthermore, the slow component decreases drastically with decreasing pH (or increasing  $H^+$  doping), especially in large-diameter tubes. We interpret this behavior as a consequence of the Burstein-Moss effect [13].

The SWNTs studied in the present work were dispersed in aqueous sodium dodecyl sulfate (SDS) surfactant, sonicated, and centrifuged. The sample preparation method was described in [6, 7]. Wavelength-dependent degenerate pump-probe measurements were performed using  $\sim 150$  fs pulses from an optical parametric amplifier (OPA) pumped by a chirped pulse amplifier (Clark-MXR CPA2010). The low pulse repetition rate (1 kHz) was ideal for reducing any thermal effects while keeping the pump fluence high. To record small photoinduced changes in probe transmission, we synchronously chopped the pump beam at 500 Hz and measured the transmission with ( $T$ ) and without ( $T_0$ ) the pump using two different gates of a box-car integrator.

Figure 1(a) shows an absorption spectrum, exhibiting three absorption bands: i) first subband ( $E_1H_1$ ) transi-

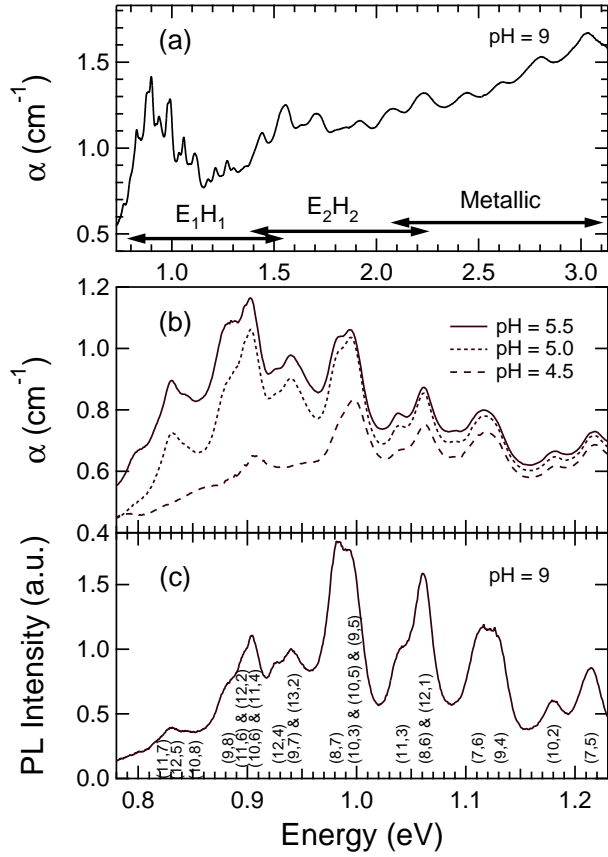


FIG. 1: (a) Linear absorption spectrum for first ( $E_1H_1$ ) and second ( $E_2H_2$ ) subband transitions in semiconducting SWNTs and first subband transitions in metallic SWNTs. (b) Linear absorption spectra in the  $E_1H_1$  range for pH = 5.5, 5.0, and 4.5. (c) Photoluminescence spectrum taken with an excitation wavelength of 632 nm.

tions in semiconducting tubes, ii) second subband ( $E_2H_2$ ) transitions in semiconducting tubes, and iii) lowest-energy transitions in metallic tubes. Figures 1(b) and 1(c) show absorption and PL in the  $E_1H_1$  range. Three traces in (b) correspond to different pH values. It is seen that absorption peaks at long wavelengths diminish with decreasing pH, similar to a recent report [14].

Figure 2(a) shows typical pump-probe data. Two traces were taken at 0.89 eV (1393 nm) and 1.60 eV (775 nm), corresponding to  $E_1H_1$  and  $E_2H_2$  transitions, respectively. Both show a positive change in transmission, i.e., photoinduced bleaching, consistent with state filling. An exponential fit reveals a fast, single decay time of 770 fs for the  $E_2H_2$  transition, consistent with intraband relaxation towards the band edge [12]. On the contrary, data in the range of  $E_1H_1$  transitions exhibit double-exponential decays. The major decay happens in the first picosecond (with decay time  $\tau_1$ ), which is followed by slower relaxation (with  $\tau_2$ ). For the particular data in Fig. 2(a), we obtain  $\tau_2 \approx 10$  ps. This long decay time has

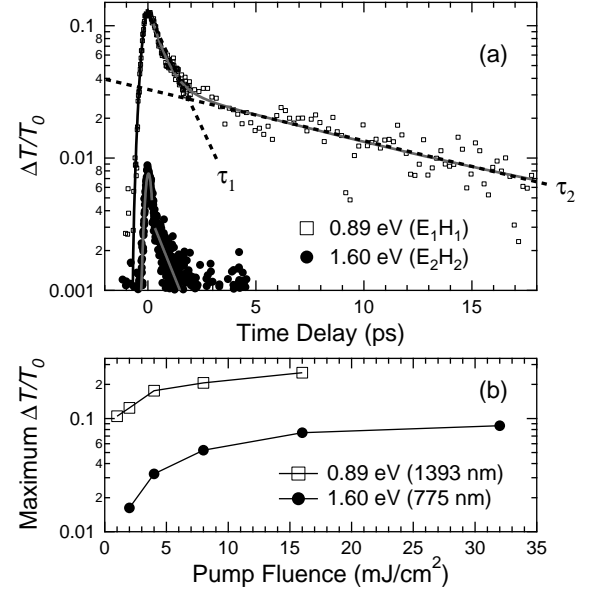


FIG. 2: (a) Pump-probe data at two wavelengths, corresponding to first and second subband transitions. (b) Maximum transmission change vs. pump fluence.

not been reported previously in either photo-emission [9] or pump-probe studies [10, 11, 12].

For both first and second subband transitions, the pump fluence dependence of the maximum value of  $\Delta T/T_0$  reveals clear saturation at high fluences, as shown in Fig. 2(b). This implies that, in the saturation regime, most of the carrier states are filled and thus the sample absorption is nearly completely quenched. A careful analysis of the differential transmission decays for 0.89 eV showed that relaxation dynamics are not dependent on the pump fluence, including the saturation regime.

To study resonant versus non-resonant excitations as well as chirality-dependent dynamics, we scanned the photon energy from 0.8 to 1.1 eV, covering the  $E_1H_1$  transitions of 0.82-1.29 nm diameter tubes [7, 8]. The fluence was kept at  $\sim 1$  mJ/cm<sup>2</sup>, below saturation [Fig. 2(b)]. Note that the probe photon energy was always the same as the pump photon energy (degenerate pump-probe spectroscopy). Figure 3(a) shows absorption, which indicates the photon energies at which we performed pump-probe measurements (labeled 1-16). Figure 3(b) shows the maximum value of  $\Delta T/T_0$  vs. photon energy; it loosely follows the absorption in (a). Shown in Fig. 3(c) is the ratio of the slow component ( $\Delta T/T_0$  at 5 ps) to the fast component ( $\Delta T/T_0$  at 0 ps); it also follows the absorption in (a), indicating that the *slow component is resonantly enhanced at absorption peaks*. Examples are shown in Figs. 3(d)-3(g). The chosen photon energies correspond to 2, 3, 11, and 13 in (a). The slow component is clearly observable only at absorption peaks.

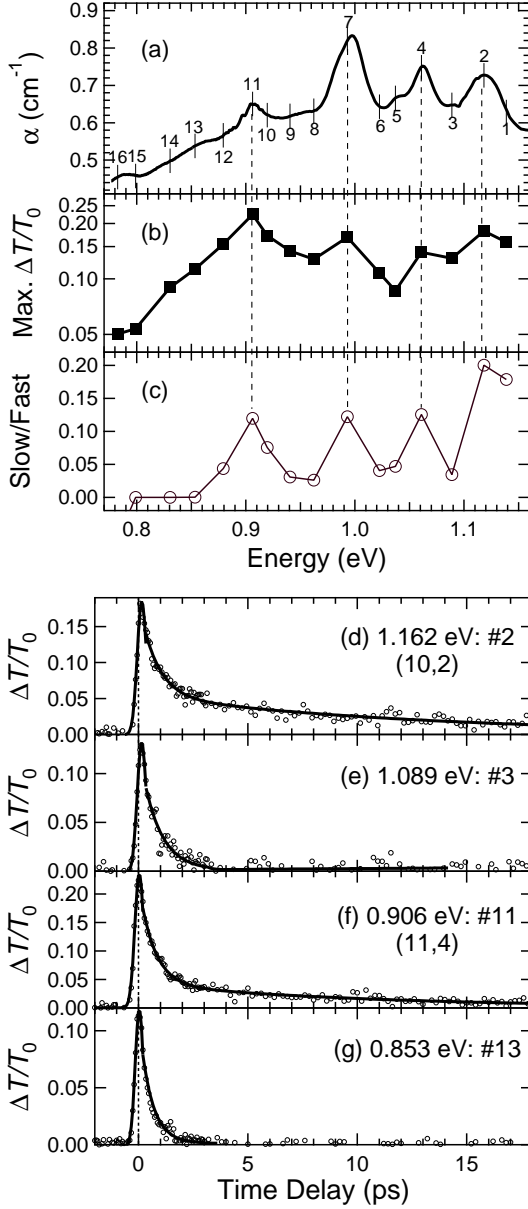


FIG. 3: (a) Linear absorption. The numbers correspond to the energies at which pump-probe measurements were made. (b) The peak value of  $\Delta T/T_0$  and (c) the ratio of slow to fast components vs. photon energy. (d)-(g): Pump-probe data taken at absorption peaks and valleys.

We also found that pump-probe dynamics are strongly dependent on the pH of the solution and the dependence is stronger at longer wavelengths (or larger tube diameters). Specifically, we observed that the slow component drastically diminishes as the pH is reduced. Examples are shown in Fig. 4. As shown in Fig. 1(b) and [14], adding hydrogen ions,  $H^+$ , to the solution (or, equivalently, decreasing the pH value) diminishes, and finally collapses, linear absorption peaks. This effect starts from the longer

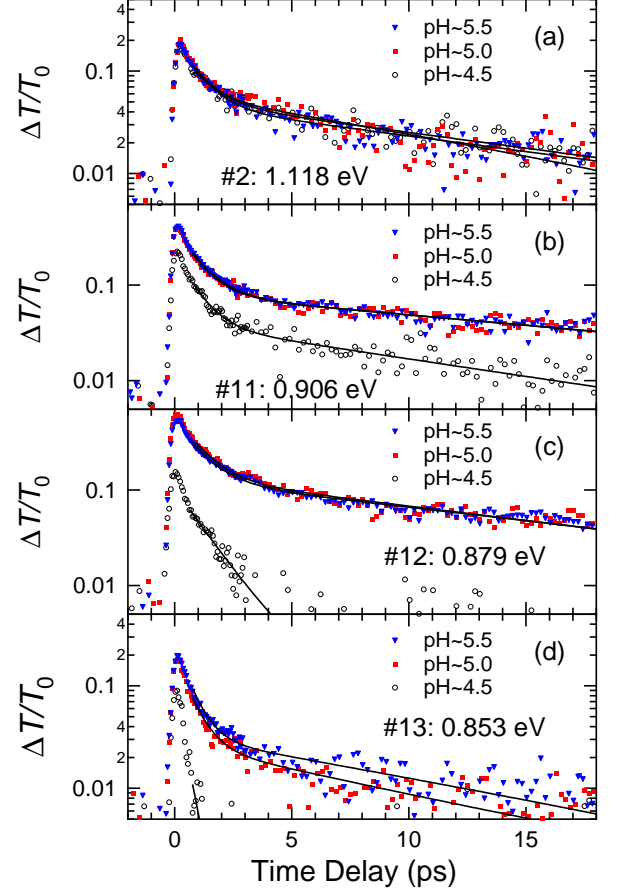


FIG. 4: pH-dependent pump-probe data for different wavelengths. The pH dependence becomes stronger for smaller photon energies (or larger-diameter tubes).

wavelength side, i.e., from larger diameter tubes. The corresponding reduction and disappearance of the slow component shows exactly the same trend (see Fig. 4).

We believe that the key to understanding the two-component decay is the co-existence of different types of tubes, i.e., sample inhomogeneity. Even when the pump photon energy resonates with one tube type, *all the other tubes with smaller band gaps are non-resonantly excited at the same time*. Thus, the pump-induced absorption bleaching due to state filling can relax in two different ways: i) intraband relaxation towards the band edge in the non-resonantly-excited tubes and ii) interband recombination in the resonantly-excited tubes. Process i) is fast (as evidenced in the  $E_2H_2$  case and in [10, 11, 12]) and always exists, irrespective of the pump wavelength, unless we resonantly excite the smallest-bandgap tubes within the diameter distribution in the sample. In addition, it is likely that there is some coherent contribution to the pump-probe signal in the fast component. However, since we have not observed any four-wave mixing signal, we do not have an estimate on the dephasing

time and thus the magnitude of this contribution. On the other hand, Process ii) is resonantly enhanced when the pump photon energy coincides with the absorption peak of one tube type since such resonantly created carriers occupy states at/near the band edge and do not have lower-energy intraband states to relax into.

There is an *intimate relationship between PL and the slow decay component*. In the previous work [10, 11, 12] neither PL nor the slow component was observed whereas our sample exhibits PL peaks at the same energies as  $E_1H_1$  absorption peaks. In addition, PL and absorption peaks diminish with decreasing pH with a concomitant abrupt disappearance of the slow decay (see Fig. 1, Fig. 4, and [14]). These facts lead us to believe that our pump-probe dynamics probes *radiative* carrier recombination. The slow decay times  $\tau_2$  should be viewed as the lower boundary of the possible range of the radiative lifetimes,  $\tau_r$ , of SWNTs. The upper limit of  $\tau_r$  depends on the rates of non-radiative recombination. Although the ratio of radiative to non-radiative rates can in principle be estimated from the quantum yield  $\eta$ , there have been no definitive studies of  $\eta$  in micelle-suspended SWNTs. The difficulty in determining  $\eta$  comes from the simultaneous occurrence of absorption by different types of tubes for a given excitation photon energy. Furthermore, very recent work has demonstrated that  $\eta$  strongly varies with the type of surfactants used [15]. Hence, precise determination of  $\tau_r$  requires understanding of the co-existing non-radiative carrier recombination processes.

There are non-radiative processes that we can rule out: first, we are not seeing any pump-power-dependent decay times, which excludes nonlinear, non-radiative recombination, i.e., Auger recombination. Second, the contact and electronic coupling between different tubes could make the system “gapless”; carriers that are supposedly created in semiconducting tubes could then recombine through purely intraband relaxation pathways due to the existence of continuum states between the conduction and valence bands as a result of interaction with metallic tubes. However, tube-tube interaction is minimized in our SDS-suspended SWNTs as evidenced by many peaks in linear spectra (Fig. 1), so this can be excluded as well. Finally, recombination on the catalyst particles at the tube ends can be ruled out since cut tube samples still show the same PL properties. One possible scenario is non-radiative recombination via surface defects in incompletely-micelle-covered nanotubes; this is conceivable in view of the surfactant-dependent radiative efficiency [15]. It should be noted that SDS shows the most prominent pH dependence while other anionic surfactants do not show the same effect. In other words, the nature of the surfactant plays an important role in the surface chemistry, and thus could influence non-radiative recombination rates. Further investigations are necessary to elucidate the origins of non-radiative recombination.

Finally, we discuss the intriguing pH dependence. The

main effect of a decreasing pH (or an increasing  $H^+$  concentration) on pump-probe data is to destroy the slow relaxation component. This process begins to occur at a larger pH for a longer wavelength (or a larger diameter tube). We attribute this to the entrance of the Fermi energy into the valence band. Adsorbed  $H^+$  ions act as acceptors, making the tubes *p*-type. When the density of such acceptors is high, the Fermi energy can go into the valence band, destroy the interband absorption peak, and thereby disable the mechanism for resonantly enhancing the slow relaxation component. This can be viewed as a 1-D manifestation of the well-known Burstein-Moss effect [13]. It is important to note that wider tubes have smaller effective masses, and therefore smaller acceptor binding energies; this explains why larger-diameter tubes are more easily affected by a pH decrease.

In summary, we have observed novel two-component dynamics in pump-probe spectroscopy experiments of SDS-suspended SWNTs. We attribute the previously-unobserved slow component (5-20 ps) to interband carrier recombination, which is resonantly enhanced whenever the pump photon energy coincides with the absorption peak of one tube type. The fast component (0.3-1.2 ps) is always present and we attribute it to intraband relaxation in non-resonantly-excited tubes. The slow component diminishes drastically with decreasing pH, as a result of the Burstein-Moss effect.

We gratefully acknowledge support from the Robert A. Welch Foundation (Grant No. C-1509), the Texas Advanced Technology Program (Project No. 003604-0001-2001), and the National Science Foundation CAREER Award (Grant No. DMR-0134058).

---

\* Author to whom correspondence should be addressed; Electronic address: kono@rice.edu

- [1] See, e.g., R. Loudon, Am. J. Phys. **27**, 649 (1959); R. J. Elliot and R. Loudon, J. Phys. Chem. Solids **8**, 382 (1959); T. Ogawa and T. Takagahara, Phys. Rev. B **43**, 14325 (1991); B. Y.-K. Hu and S. Das Sarma, Phys. Rev. Lett. **68**, 1750 (1992); T. Ando, J. Phys. Soc. Jpn. **66**, 1066 (1997).
- [2] *Carbon Nanotubes*, eds. M. S. Dresselhaus *et al.* (Springer, Berlin, 2001).
- [3] H. Ajiki and T. Ando, J. Phys. Soc. Jpn. **62**, 1255 (1993); W. Tian and S. Datta, Phys. Rev. B **49**, 5097 (1994); J. P. Lu, Phys. Rev. Lett. **74**, 1123 (1995).
- [4] O. E. Alon *et al.*, Phys. Rev. Lett. **85**, 5218 (2000).
- [5] H. Kataura *et al.*, Synth. Metals **103**, 2555 (1999); S. Kazaoui *et al.*, Phys. Rev. B **60**, 13339 (1999); J. Hwang *et al.*, Phys. Rev. B **62**, R13310 (2000).
- [6] M. J. O’Connell *et al.*, Science **297**, 593 (2002).
- [7] S. M. Bachilo *et al.*, Science **298**, 2361 (2002).
- [8] R. B. Weisman and S. M. Bachilo, Nano Lett. **3**, 1235 (2003).
- [9] T. Hertel and G. Moos, Phys. Rev. Lett. **84**, 5002 (2000).
- [10] Y. C. Chen *et al.*, Appl. Phys. Lett. **81**, 975 (2002).

- [11] H. Han *et al.*, Appl. Phys. Lett. **82**, 1458 (2002).
- [12] J. S. Lauret *et al.*, Phys. Rev. Lett. **90**, 057404 (2003).
- [13] E. Burstein, Phys. Rev. **93**, 632 (1954); T. S. Moss, Proc. Phys. Soc. (London) B **67**, 775 (1954).
- [14] M. S. Strano *et al.*, J. Phys. Chem. B **107**, 6979 (2003).
- [15] V. C. Moore *et al.*, Nano Lett. **3**, 1379 (2003).